In situ simultaneous synthesis of WC/graphitic carbon nanocomposite as a highly efficient catalyst support for DMFC

Ruihong Wang, Chungui Tian, Lei Wang, Baoli Wang, Hengbin Zhang Honggang Fu*

Key Laboratory of Functional Inorganic Material Chemistry

(Heilongjiang University), Ministry of Education,

Heilongjiang University, Harbin 150080 P. R. China.

Tel.: +86 451 8660 8458;

fax: +86 451 8667 3647;

E-mail: fuhg@vip.sina.com.

Supporting Information

Experimental:

1. The basic structure of the ion exchange resin used in the synthesis

The basic structure of commercial polyacrylic weak-base anion exchange resin is shown in Fig. S1. The resin network exists of poly-methyl acrylate chain segments that react with polyethylene polyamine followed by chlorination to get this weak-base anion exchange resin. The Cl^- ions in this polymer can be exchanged by other anions.

2. Preparation of the WC/GC nanocomposite

In a typical preparation, 10 g weak-base anion exchange resins were impregnated with 85 ml of 0.15 mol L^{-1} mixed solution containing Na_2WO_4 and $K_4[Fe(CN)_6]$ (mole ratio 1:1), forming resin-WO_4^{2-}-$[Fe(CN)_6]^{4-}$ complex. The resulting product was washed with deionized water, dried at 100 ℃ for 12 h in an oven and carbonized at 1000 ℃ with a heating rate of 5 K/min under highly pure N_2 flow and maintained at that temperature for 1 h. After slow cooling to room temperature, black product was obtained. Subsequently, the resulting product was ground into power and treated with excessive HCl solution to remove Fe species. The final product was denoted as WC/GC (GC is for graphitic carbon).

3. Synthesis of WC_{1-x}/AC and GC

10 g weak-base anion exchange resins were impregnated respectively in 200 mL of 0.1 mol L^{-1} Na_2WO_4 and 100 mL of 0.1 mol L^{-1} $K_4[Fe(CN)_6]$ aqueous solution to get the corresponding derivatives, denoted as resin-WO_4^{2-} and resin-$[Fe(CN)_6]^{4-}$. Tungsten carbide/amorphous carbon (WC_{1-x}/AC) and graphitic carbon (GC) were prepared respectively by heating treatment of resin-WO_4^{2-} and resin-$[Fe(CN)_6]^{4-}$ respectively. The synthetic procedure was same with that for preparation of WC/GC.

4. Synthesis of WC-GC (Wet-impregnation) and WC+GC (mechanical-mix)

Wet-impregnation method: In this strategy, the composite of WC and GC denoted as WC-GC (Wet-impregnation) was prepared via a conventional two-step process. In a typical preparation, 0.440 g ammonium paratungstate $(NH_4)_6W_7O_{24}$ was dissolved in 50 ml of deionized water and followed by adding 0.380 g GC. The weight content of tungsten was 47.1 wt% as same as that in WC/GC prepared *via* in-situ simultaneous route. This mixture was stirred vigorously at 70℃ for 2 h to realize complete wetting of carbon and impregnation of tungsten ions. Then the solvent was fast evaporated at 100℃ under continuous stirring. The resulting solid was further dried at 70℃ for 6 h in a vacuum oven and then calcinated at 450℃ for 2h (Step I). In succession, this solid was carbonized at 800℃ with a heating rate of 5 K/min under a CO stream (flow rate: 180 ml/min) and maintained at 800℃ for 8 h (Step II). After slow cooling to room temperature, the final product was obtained. The XRD patterns of products obtained in Step I and Step II are shown in Fig. S9.

Mechanical-mix method: WC+GC (mechanical-mix) was obtained by mechanically mixing of WC and GC. In the preparation, 0.372 g pure WC power obtained by an unpublished method in our lab was mechanically mixed with 0.380 g GC. The weight content of tungsten in WC+GC (mechanical-mix) sample is 47.1 wt%. The corresponding XRD of sample is shown in Fig. S10.

5. The tests about the amount of tungsten in resin and products

After ion exchange resin was saturated by impregnating in corresponding salt aqueous solution for 24 h, the residual solution was analyzed by atomic absorption spectrometer (AAS) to measure the amount of exchanged anions. After carbonization, weight method was used to measure the amount of tungsten in the products. The results show the weight percentage of tungsten in WC/GC and WC_{1-x}/AC was 47.1 wt% and 75.6 wt%, respectively.

6. Preparation of electrocatalysts

WC/GC-supported Pt catalyst was prepared by conventional $NaBH_4$ reduction method. Typically, 200 mg of WC/GC composite was suspended in deionized water and ultrasonicated to form dispersed slurry. The slurry was added into H_2PtCl_6 solution with Pt concentration of 2 mM. The loading of Pt was adjusted to be 7.5 wt%. Excessive Na_2BH_4 solution was added into the mixed solution under vigorously stirring for 2 h at ambient temperature. Then the product was settled for overnight and filtered, rinsed thoroughly with deionized water, and then freezed-dried. The final product was named as Pt-WC/GC. Similarly, WC_{1-x}/AC, GC, WC-GC (Wet-impregnation) and WC+GC (mechanical-mix) supported Pt catalysts (Pt-WC_{1-x}/AC, Pt-GC, Pt-WC-GC (Wet-impregnation) and Pt-WC+GC (mechanical-mix)) were also synthesized as the same procedures. In addition, Vulcan carbon supported Pt catalyst (Pt-VC) with Pt loading of 20 wt% is fabricated for comparison.

Characterization:

1. Physical characterizations

Powder X-ray diffraction (XRD) patterns were displayed in a Rigaku D/max-IIIB diffractometer (operating at 40 kV and 20 mA,) with a scanning rate of 4° min^{-1} using Cu K_{α} radiation ($\lambda = 1.5406$ Å). Transmission electron microscopy (TEM) measurements were carried out on a JEOL-3010 transmission electron microscopy at an operating voltage of 200 kV. Raman spectra were performed on a Jobin Yvon HR 800 micro-Raman spectrometer at 457.9 nm. The atomic absorption spectroscopy was measured on Thermo Elemental SOLAAR. The thermal pyrolysis experiment was carried out in a TG thermobalance (TA SDTQ600). The resin-WO_4^{2-}-$[Fe(CN)_6]^{4-}$ complex powder of around 20 mg was heated from 30 to 1000 □ at 5 □/min in N_2 atmosphere with a flow rate of 60 ml/min (The condition for TG test was set as same as the parameters of synthetic experiment). Nitrogen adsorption–desorption isotherms at 77 K were collected on a Tristar 3000 nitrogen adsorption apparatus. The Brunauer–Emmett–Teller (BET) equation was used to calculate the specific surface area. Pore size distributions were obtained using the Barrett–Joyner–Halenda (BJH) method from the adsorption branch of the isotherm.

2. Electrochemical measurements

Electrochemical activity and stability of catalysts to methanol oxidation were evaluated by BAS100B electrochemical workstation. Electrochemical Impedance Spectra (EIS) were performed with a computer-controlled IM6e Impedance Analyzers at ambient temperature. The conventional three-electrode cell consisting of glassy carbon electrode with an area of 0.16 cm^2 as the working electrode, Pt plate as the counter electrode, and saturated Ag/AgCl electrode as reference electrode was used. All the electrochemical measurements were carried out in an mixed aqueous solution of 1.0 M H_2SO_4 and 1.0 M CH_3OH. The catalyst ink was prepared by dispersing 5 mg of catalyst in 0.1 ml 2-propanol and 30 µl Nafion solution (5 wt% Aldrich). The mixture was ultrasonicated for 30 min, then 10 µl of the suspension was dropped onto the pre-cleaned glassy carbon electrode and the solvent was slowly evaporated. The catalyst loading for each electrode was 2.40 mg cm^{-2}. Cyclic voltammetry (CV) measurements were carried out between the potential range of -0.2 and 1.0 V at a scan rate of 50 mV s^{-1}. The Chronoamperometry test (CA) for catalyst was measured with the potential fixed at 0.7 V for 3600s. EIS were scanned by applying sinusoidal perturbations of 10 mV at the frequency range from 100 KHz to 10 mHz. Prior to electrochemical experiments, the electrolytic solution was purged with high-purity N_2 for 0.5 h to remove the dissolved oxygen.

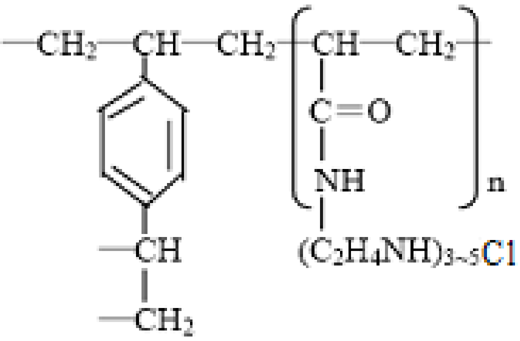

Fig. S1 The basic structure of polyacrylic weak-base anion exchange resin.

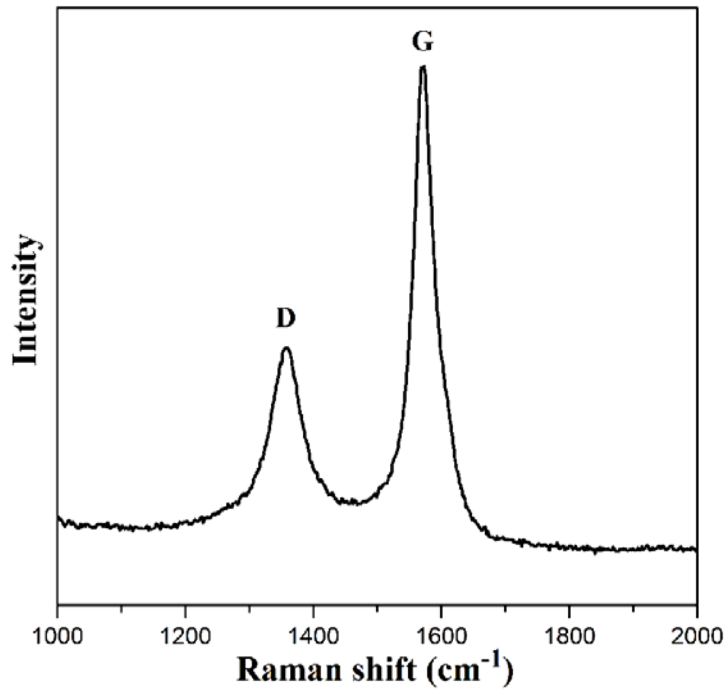

Fig. S2 Raman spectrum of WC/GC.

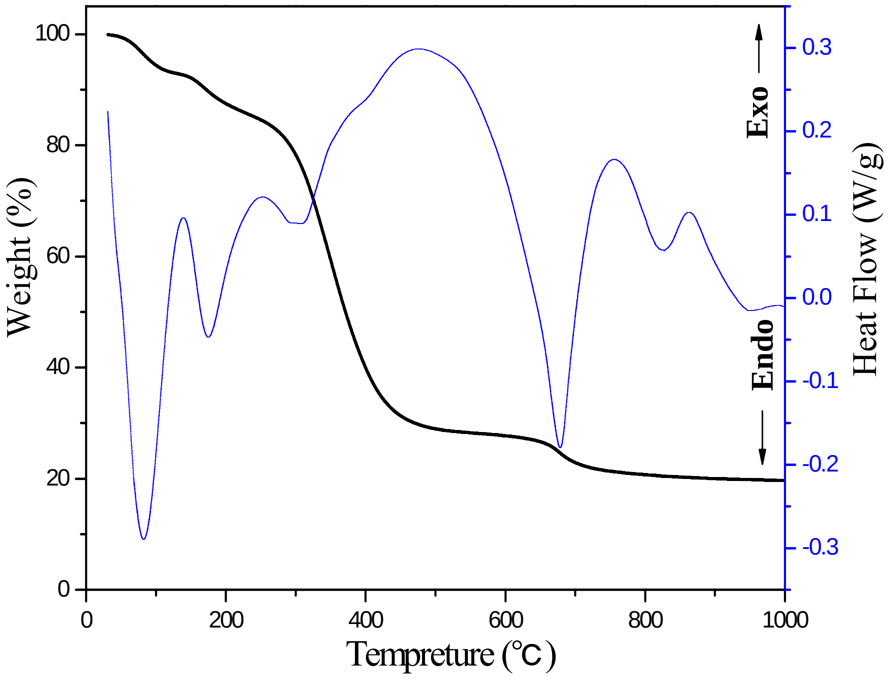

Fig. S3 TG-DSC curves for thermal pyrolysis of resin-WO_4^{2-}-$[Fe(CN)_6]^{4-}$ complex.

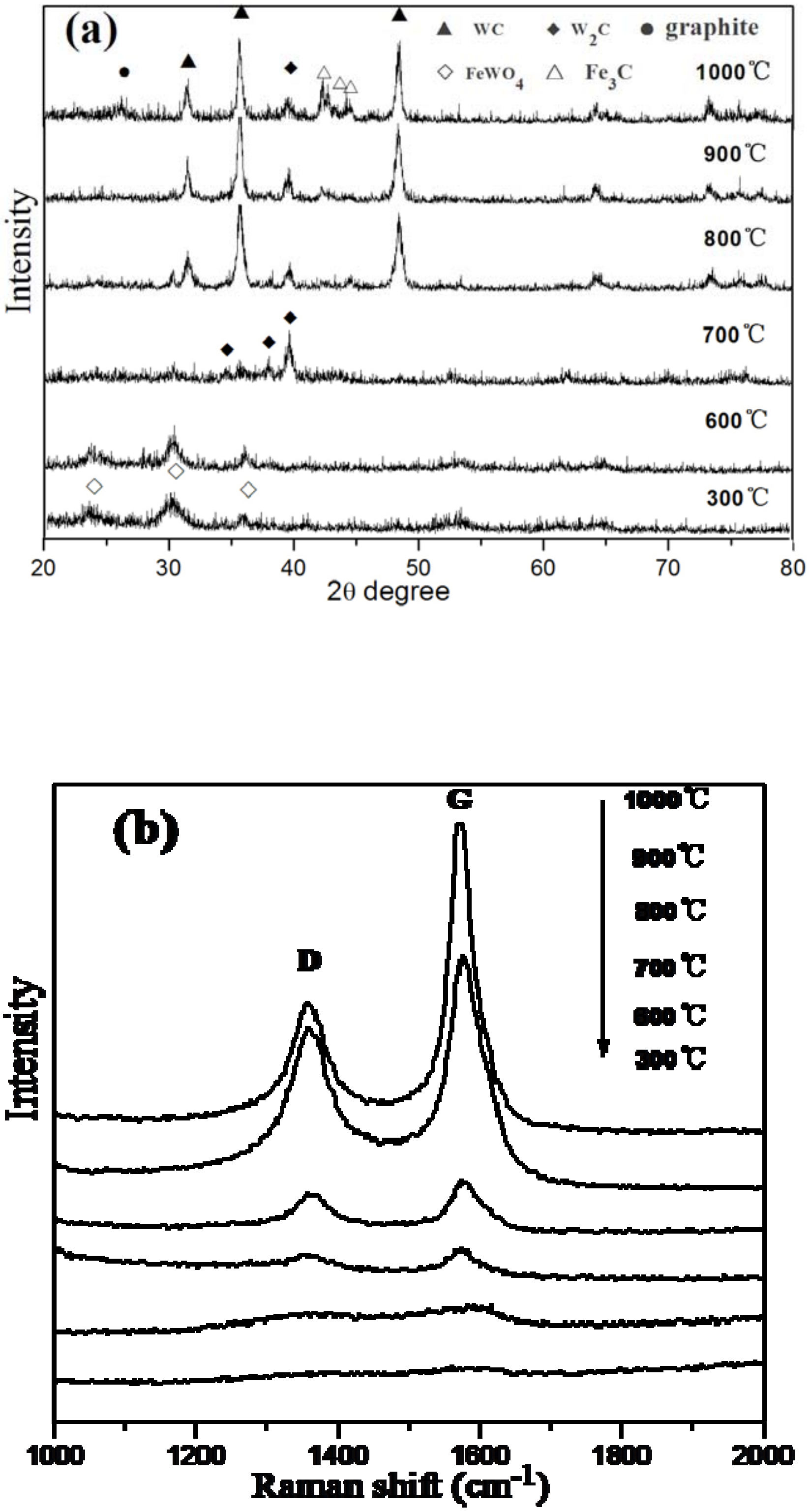

Fig. S4 XRD patterns (a) and Raman spectra (b) of samples derived from resin-WO_4^{2-}-$[Fe(CN)_6]^{4-}$ complex after carbonization at different temperatures.

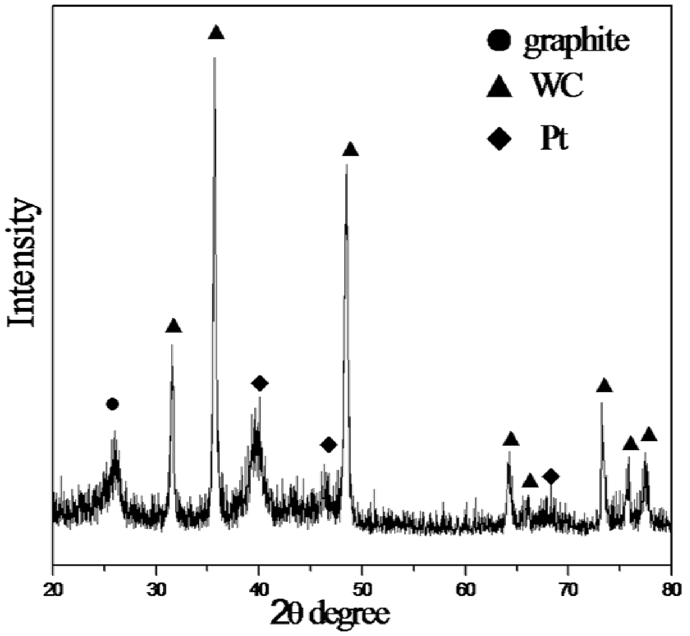

Fig. S5 XRD pattern of Pt–WC/GC.

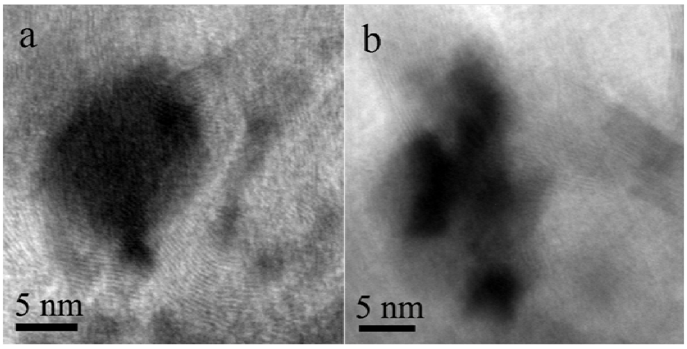

Fig. S6 HRTEM images of (a) WC particle and (b) Pt particles obtained from the TEM image of Pt-WC/GC (Fig. 1D in manuscript).

Two kinds of typical particles with different size could be observed from the sample Pt-WC/GC (Fig. 1D in the manuscript). The HRTEM images for such particles are shown in Fig. S6a and Fig. S6b. Comparing the particle size with WC in sample WC/GC (Fig. 1B in the manuscript), we speculate the particle with size of ~10 nm in Fig. S6a should be WC. And another typical particles in Fig. S6b with size about 4 nm should be Pt particles by combining TEM with XRD analysis (Debye-Scherrer equation).

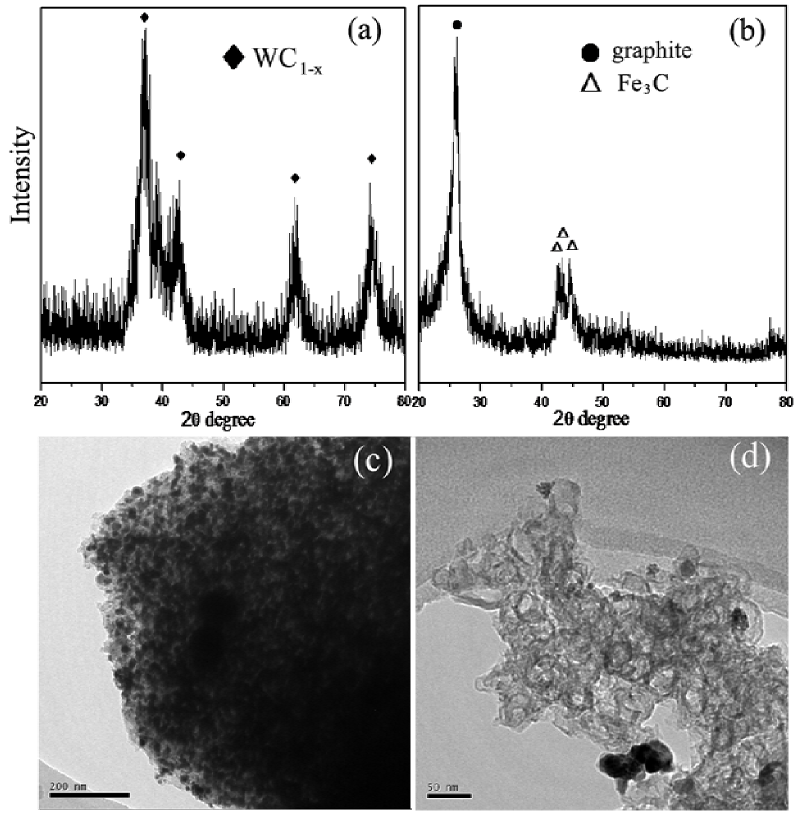

Fig. S7 XRD patterns of WC_{1-x}/AC (a) and GC (b), TEM images of WC_{1-x}/AC (c) and GC (d).

The X-ray diffraction pattern of WC_{1-x}/AC was shown in Fig. S7(a). The diffraction peaks at 36.9°, 42.9°, 62.0° and 74.2° can be assigned as (111), (200), (220) and (311) planes of WC_{1-x}, respectively. No diffraction peak of graphitic carbon was observed, suggesting that carbon in the composite is amorphous. TEM image of sample WC_{1-x}/AC in Fig. S7(c) shows that WC_{1-x} particles are well-dispersed in carbon phase with the average size of nanoparticles around 10 nm. In the case of sample GC (see Fig. S7(b)), the intensive diffraction peaks at 26.2° for graphite (002) plane is detected, demonstrating carbon in GC is well graphitized. Also, the diffraction peaks of Fe_3C exist after removal of Fe species, which can be explained by the fact that Fe_3C is a co-feeding compound with carbon phase and difficult to eliminate thoroughly. Fig. S7(d) displays the TEM image of sample GC, which is mainly consisted of carbon nanocapsules.

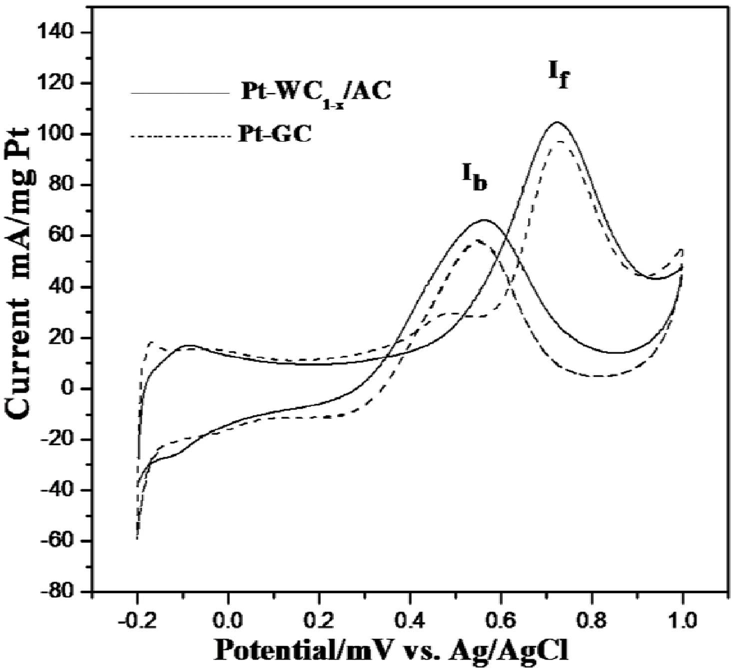

Fig. S8 Cyclic voltammograms of methanol oxidation at Pt-WC_{1-x}/AC and Pt-GC catalysts after the current was stable.

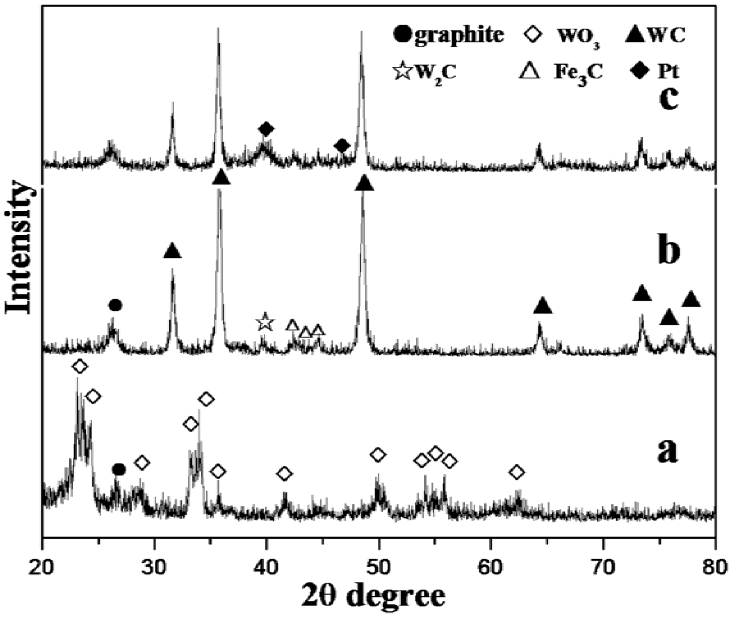

Fig. S9 XRD patterns of (a) WO_3-GC, (b) WC-GC (wet-impregnation) and Pt-WC-GC (wet-impregnation)

Fig. S9 shows the XRD patterns of products obtained from wet-impregnation method. The results shows that the the tungsten species were transformed into WO_3 (Fig. S9a) after calcinated at 450□for 2h (Step I), and into WC (Fig. S9b) after carbonized at 800□for 8 h

(Step II). Therefore, the tungsten species undergoes a phase changes as the sequence: tungstate→WO_3→WC. In the XRD pattern shown in Fig. S9c, the peaks at 2θ = 39.8°, 46.2°are characteristic of face-centered cubic Pt, confirming the formation of Pt nanoparticles.

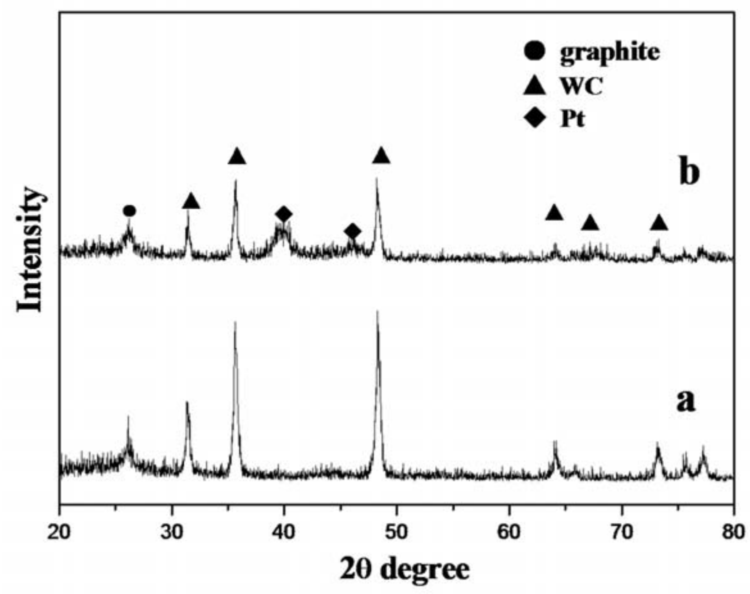

Fig. S10 XRD patterns of (a) WC+GC (mechanical-mix) and (b) Pt-WC+GC (mechanical-mix)

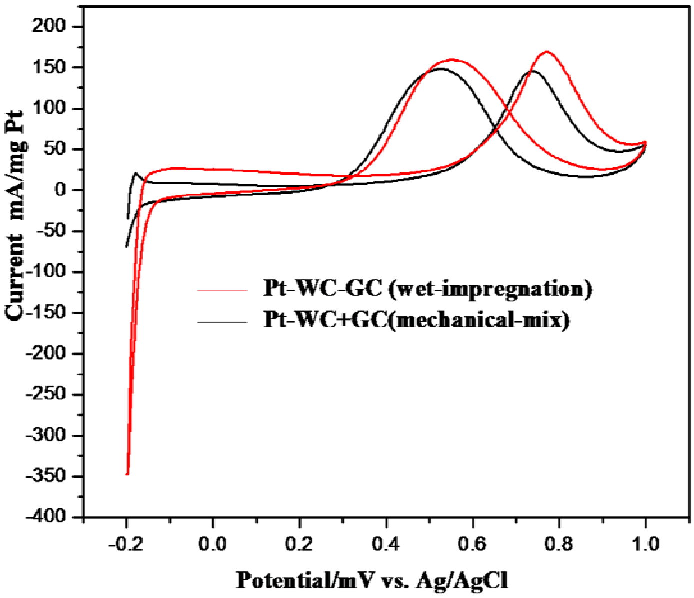

Fig. S11 Cyclic voltammograms for methanol oxidation of Pt-WC/GC, Pt-WC-GC (wet-impregnation) and Pt-WC+GC (mechanical-mix).

Fig. S11 shows the steady-state Cyclic voltammograms of two catalysts, also the peak current densities and potentials of the forward scan for different samples are also listed in Table

S1.

Table S1. Electrochemical measurements of Pt-WC-GC (wet-impregnation) and Pt-WC+GC(mechanical-mix)

Catalyst	Mass activity (mA mg^{-1} Pt)	Peak Potential (v)
Pt-WC-GC(wet-impregnation)	171.2	0.773
Pt-WC+GC(mechanical-mix)	142.6	0.736

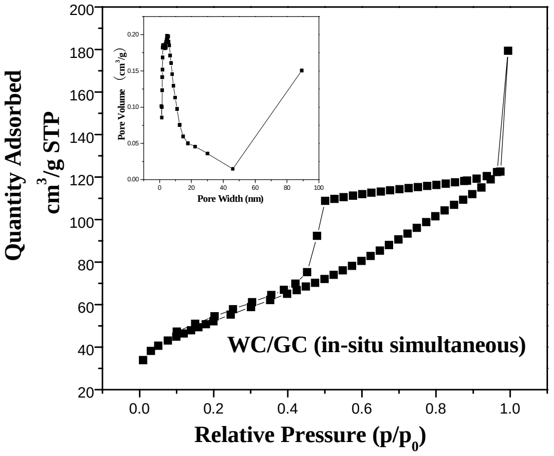

Fig. S12 N_2 adsorption/desorption isotherm of WC/GC (in-situ simultaneous synthesis) and the inset indicates pore-size distribution obtained by the BJH method.

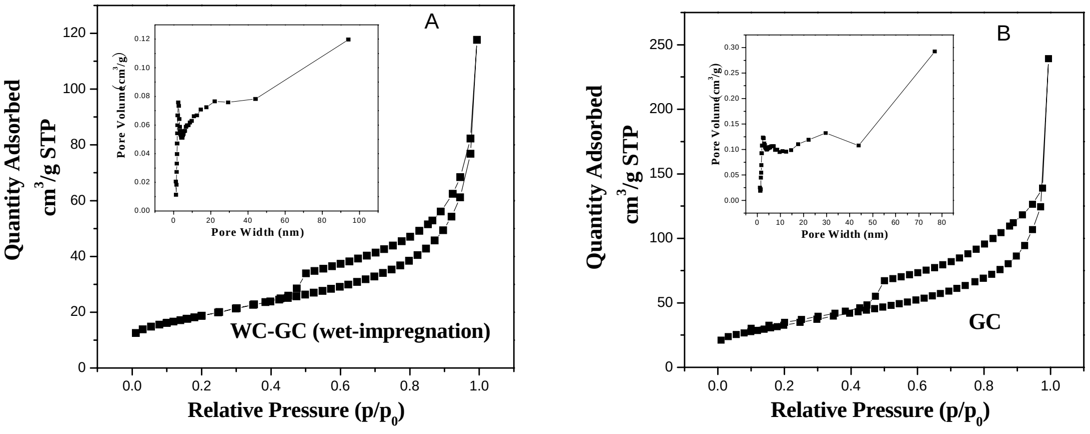

Fig. S13 (A) N_2 adsorption/desorption isotherm of WC-GC (wet-impregration) and the inset indicates pore-size distribution obtained by the BJH method; (B) N_2 adsorption/desorption isotherm of GC and the inset indicates pore-size distribution obtained by the BJH method.

For studying the pore structures of samples obtained by different methods and understanding their influence on the catalytic performance, the BET and porosity of WC/GC (in-situ simultaneous synthesis), WC-GC (wet-impregnation) as well as GC are provided and analyzed in detail (see Fig. S12, Fig. S13).

As shown in Fig. S12, WC/GC (in-situ simultaneous synthesis) exhibits a typical Type IV isotherm similar with H2 hysteresis and the pore-size distribution of WC/GC is mainly in the region of 2~5 nm. The SSA and total pore volume of sample are 155 m^2/g, 0.219 cm^3/g, respectively. In comparison, both the samples of GC and WC-GC (wet-impregnation) give a similar hysteresises with broad and uneven pore-size distribution (Figure S13), which are obviously different from that of WC/GC (in-situ simultaneous synthesis). The SSA and total pore volume of GC and WC-GC (wet-impregnation) are 116 m^2/g, 0.374 cm^3/g and 66 m^2/g, 0.185 cm^3/g, respectively. Clearly, the SSA and pore volume of the latter are much lower than those of the former (GC), which should be ascribed to the wet-impregnation route. In such a way, the aggregation or sintering of WC particles often occur, leading to the jam of porous structure. The results of BET and N_2 adsorption isotherms clearly indicate that the in-situ simultaneous route is beneficial to improve SSA and porosity of WC/GC composite, which should be in favor of the improved catalytic performance.